2013

ESPI filtering method based on anisotropic coherence diffusion and Perona-Malik diffusion

Zhitao Xiao
Tianjin University of Technology,Tianjin Polytechnic University,Institute of Molecular and Cell Biology

Zhenbei Xu
Tianjin Polytechnic University

Fang Zhang
Tianjin University of Technology

Lei Geng
Tianjin University, Tianjin, China

Jun Wu
Tianjin University of Technology, zhenkongwujun@163.com

See next page for additional authors

ESPI filtering method based on anisotropic coherence diffusion and Perona-Malik diffusion

Abstract

Noise reduction is one of the most important concerns in electronic speckle pattern interferometry (ESPI). According to partial differential equation (PDE) filtering theory, we present an anisotropic PDE noise-reduction model based on fringe structure information for interferometric fringe patterns. This model is based on coherence diffusion and Perona-Malik (P-M) diffusion. The former can protect the structure information of fringe pattern, while the latter can effectively filter off the noise inside the fringes. The proposed model generated by the two diffusion methods helps to obtain good effects of denoising and fidelity. ESPI fringes and the phase pattern are tested. Experimental results validate the performance of the proposed filtering model.

Disciplines

Engineering | Science and Technology Studies

Authors

Zhitao Xiao, Zhenbei Xu, Fang Zhang, Lei Geng, Jun Wu, Quan Yuan, and Jiangtao Xi

ESPI filtering method based on anisotropic coherence diffusion and Perona-Malik diffusion

Zhitao Xiao (肖志涛)[1], **Zhenbei Xu (徐振北)**[1], **Fang Zhang (张　芳)**[1*], **Lei Geng (耿　磊)**[1],
Jun Wu (吴　骏)[1], **Quan Yuan (袁　泉)**[1], and **Jiangtao Xi (习江涛)**[2]

[1]*School of Electronics and Information Engineering, Tianjin Polytechnic University, Tianjin 300387, China*

[2]*School of Electrical, Computer, and Telecommunications Engineering, University of Wollongong,*

Wollongong, NSW 2522, Australia

*Corresponding author: hhzhangfang@126.com

Noise reduction is one of the most important concerns in electronic speckle pattern interferometry (ESPI). According to partial differential equation (PDE) filtering theory, we present an anisotropic PDE noise-reduction model based on fringe structure information for interferometric fringe patterns. This model is based on coherence diffusion and Perona-Malik (P-M) diffusion. The former can protect the structure information of fringe pattern, while the latter can effectively filter off the noise inside the fringes. The proposed model generated by the two diffusion methods helps to obtain good effects of denoising and fidelity. ESPI fringes and the phase pattern are tested. Experimental results validate the performance of the proposed filtering model.

OCIS codes: 110.6150, 030.6140, 100.3008.

doi: 10.3788/COL201311.101101.

Electronic speckle pattern interferometry (ESPI) is a non-destructive optical measurement technique, which is widely used in deformation measurement and nondestructive testing of rough surface[1,2]. Accurate extraction of phase from fringe patterns is of fundamental importance for the successful application of ESPI in obtaining displacement. However, strong grain-shaped random noise in the fringe patterns usually leads to significant errors in phase extraction. To reduce measurement errors, the inherent noise of fringe patterns should be removed in ESPI[3].

The method based on partial differential equation (PDE) is widely used in image processing and computer vision. This technique changes image according to a specified PDE, and the solution of the PDE is the processed result[4]. Perona *et al.*[5] proposed a nonlinear diffusion model, which they named Perona-Malik (P-M) diffusion. This model can protect the edges in image denoising, which gives a fresh direction for subsequent applications of PDEs in image processing. Weickert[6] constructed a coherent enhancement model, which introduced structure tensor to denote the local structure information of an image and achieves good filtering results for fingerprint image.

In this letter, the advantages and disadvantages of P-M diffusion and coherent enhancement models in ESPI are analyzed. Based on anisotropic tensor and P-M diffusions, a PDE denoising model is established. The effectiveness of the proposed method in ESPI is tested on computer-simulated and practically captured fringes.

Let u_0: $R^2 \rightarrow R$, where $u_0(x, y)$ is the gray-level of pixel (x, y), which represents a gray-level image to be processed. The image deforms with time t as

$$\frac{\partial u}{\partial t} = F[u(x,y,t)], \quad u(x,y,0) = u_0(x,y), \qquad (1)$$

where $u(x, y, t)$: $R^2 \times [0, \tau] \rightarrow R$ is the evolving image;

F: $R \rightarrow R$ is an operator that depends on the purpose of processing, such as denoising, enhancement, and segmentation; the image u_0 is the initial condition. The solution $u(x, y, t)$ of Eq. (1) gives the processed image.

Perona *et al.*[5] obtained denoised image by solving the following diffusion equation:

$$\begin{cases} \dfrac{\partial u}{\partial t} = \mathrm{div}(g(|\nabla u|)\nabla u) \\ u(x,y,0) = u_0(x,y) \end{cases}, \qquad (2)$$

where ∇u is the gradient of the evolving image u with respect to the filtered result, and g is a smooth non-increasing function with $g(|\nabla u|) = k^2/(k^2 + |\nabla u|^2)$, in which k is a constant parameter. Smoothing is performed based on the following assumptions. If the value of $\nabla u(x, y)$ is large, (x, y) will be located at the edge of the image. Then, the diffusion will be slow, and the exact localization of the edges will be maintained. However, if the value of $\nabla u(x, y)$ is small, (x, y) will be located in the flat region, then the diffusion will tend to be smoother around (x, y). g evidently influences the diffusion speed. Therefore, minimal smoothing is acquired around the edge of the image. Although Perona *et al.* made significant improvement on the theory and obtained better filtering result, Eq. (2) was still isotropic around the local area of each pixel. In addition, the problem of edge blurring is unavoidable.

Weickert introduced the structure tensor matrix, through which richer local structure information can be obtained[7]. An anistropic tensor diffusion model is produced based on the structure information of an image. The structure tensor matrix **J** is defined as

$$\mathbf{J} = \begin{vmatrix} j_{11} & j_{12} \\ j_{21} & j_{22} \end{vmatrix}$$

$$= \begin{vmatrix} \left(\dfrac{\partial u_\sigma}{\partial x}\right)^2 * G_\rho & \left(\dfrac{\partial u_\sigma}{\partial x}\dfrac{\partial u_\sigma}{\partial y}\right) * G_\rho \\ \left(\dfrac{\partial u_\sigma}{\partial x}\dfrac{\partial u_\sigma}{\partial y}\right) * G_\rho & \left(\dfrac{\partial u_\sigma}{\partial y}\right)^2 * G_\rho \end{vmatrix}, \quad (3)$$

where u_σ represents the smoothed image by the Gaussian filter with parameter σ, and G_ρ is the Gaussian kernel function with parameter ρ.

The two eigenvalues of $\mathbf{J}$ can be represented as

$$\lambda_{1,2} = \frac{1}{2}(j_{11} + j_{22} \pm \sqrt{(j_{11} - j_{22})^2 + 4j_{12}^2}). \quad (4)$$

The eigenvectors ξ and η are

$$\xi = \frac{\nabla u}{|\nabla u|} = (\cos\theta, \sin\theta), \quad (5)$$

$$\eta = \frac{\nabla_\perp u}{|\nabla u|} = (-\sin\theta, \cos\theta), \quad (6)$$

where $\theta = \frac{1}{2}\arctan\frac{2j_{12}}{j_{11}-j_{22}}$. To characterize the structure information of an image, the coherence function is defined as

$$H = (\lambda_1 - \lambda_2)^2 = (j_{11} - j_{22})^2 + 4j_{12}. \quad (7)$$

If $\lambda_1 = \lambda_2 = 0$, then $H = 0$, which means that the gray scales near the current point vary nonsignificantly in all directions, and the current point is in the flat region of the image.

If $\lambda_1 \gg \lambda_2 = 0$, then $H \gg 0$, which signifies that the gray scales change much greater in a certain direction than that in its vertical direction, and the image has obvious edge characteristics at the current point.

If $\lambda_1 \geqslant \lambda_2 \gg 0$, then $H \geqslant 0$, which shows that the gray scales on both perpendicular directions change rapidly; therefore, corners or "T" structures exist near this point.

Hence, Weickert[6] proposed the tensor diffusion model as

$$\frac{\partial u}{\partial t} = \mathrm{div}(\mathbf{D}\nabla u), \quad (8)$$

where $\mathbf{D}$ is a 2×2 positive, definite matrix, which has the same eigenvectorsas the structure tensor $\mathbf{J}$. Hence, $\mathbf{D}$ can control the diffusion direction of the equation. To protect important structural information, such as edges and corners, the diffusion coefficients μ_1 and μ_2 along the two perpendicular directions ξ and η are identified as

$$\begin{cases} \mu_1 = \alpha \\ \mu_2 = \begin{cases} \alpha, & \lambda_1 = \lambda_2 \\ \alpha + (1-\alpha)\exp\left[\dfrac{1}{(\lambda_1 - \lambda_2)^2}\right], & \text{else} \end{cases} \end{cases}, \quad (9)$$

where α is a small positive number to protect the image edge, e.g., $\alpha = 0.00001$.

In the strong coherence areas of the image ($H \gg 0$), i.e., the image edges, $\mu_2 \approx 1$, which is close to the maximum diffusion rate and has full diffusion along the direction of η. When the image has no significant coherence, i.e., in the corners or flat areas, $H \approx 0$ and $\mu_2 \approx \alpha$, diffusion will become very slow to protect the corners.

However, the noise in the flat areas cannot be well removed.

Using Eqs. (5), (6), and (9), the elements of the matrix $\mathbf{D}$ are easily obtained as

$$\mathbf{D} = \begin{pmatrix} a & b \\ b & c \end{pmatrix}, \quad (10)$$

where

$$\begin{cases} a = \mu_1 \cos^2\theta + \mu_2 \sin^2\theta \\ b = (\mu_1 - \mu_2)\sin\theta\cos\theta \\ c = \mu_2 \cos^2\theta + \mu_1 \sin^2\theta \end{cases}. \quad (11)$$

Hence, the tensor diffusion model is inclined to diffuse along the η direction, which can repair the broken edges of the image and protrude the edge or corner features. However, an excessive drive for the structural information will lead to the problem that the diffusion equation considers the noise points in the flat region as a part of the edges, which can lead to virtual stripes in the flat region.

According to the analysis above, given that ESPI fringes have no obvious edge, the diffusion coefficient g in Eq. (2) is still large around the image edges, and a clear filtered ESPI fringe cannot be obtained by P-M diffusion model. However, the P-M equation can remove noises sufficiently in flat areas. With coherent coefficients, the tensor diffusion model has a good ability of edge-repair in image edges. However, in flat regions with small coherence, filtering is not sufficient and denoising effect is not satisfied. Thus, we propose the following diffusion equation:

$$\frac{\partial u}{\partial t} = G_1(\mu_1 u_{\xi\xi} + \mu_2 u_{\eta\eta}) + G_2\mathrm{div}(g(|\nabla u|)\nabla u), \quad (12)$$

where

$$\begin{cases} u_{\eta\eta} = \dfrac{u_{xx}u_y^2 - 2u_x u_y u_{xy} + u_{yy}u_x^2}{u_x^2 + u_y^2} \\ u_{\xi\xi} = \dfrac{u_{xx}u_x^2 + 2u_x u_y u_{xy} + u_{yy}u_y^2}{u_x^2 + u_y^2} \end{cases}, \quad (13)$$

are the second derivatives of u along the ξ and η directions, respectively, and μ_1 and μ_2 conform to Eq. (10).

In Eq. (12), the first part, depending on the coherent diffusion, can protect corners and repair edges. The second part ensures enough smoothing in flat regions. To modify the relationship of the two parts, we set $G_1 = 1 - g(|\nabla u|)$ and $G_2 = g(|\nabla u|)$. At the edge areas, $g(|\nabla u|)$ is smaller, and the first part plays a main part in diffusion to repair the edges and protect the corners. In flat regions, $g(|\nabla u|)$ is larger, and the second part plays the main role in diffusion to achieve fully smoothness.

To solve Eq. (12) numerically, the equation has to be discretized. The image is represented by $M \times N$ matrix of intensity values. For any function (i.e., image) $u(x, y)$, we thus let $u_{i,j}$ denote $u(i, j)$ for $1 < i < M$, $1 < j < N$. The evolution equations give images at $t_n = n\Delta t$. We denote $u(i, j, t_n)$ by $u_{i,j}^n$. The time derivative u_t at (i, j, t_n) is approximated by the forward difference as

$$(u_t)_{i,j}^n = \frac{u_{i,j}^{n+1} - u_{i,j}^n}{\Delta t}, \quad (14)$$

where Δt is the step-size in the time domain.

The spatial derivatives are

$$
\begin{cases}
(u_x)_{i,j}^n = \dfrac{u_{i+1,j}^n - u_{i-1,j}^n}{2} \\[2mm]
(u_y)_{i,j}^n = \dfrac{u_{i,j+1}^n - u_{i,j-1}^n}{2} \\[2mm]
(u_{xx})_{i,j}^n = u_{i+1,j}^n - 2u_{i,j}^n + u_{i-1,j}^n \\[2mm]
(u_{yy})_{i,j}^n = u_{i,j+1}^n - 2u_{i,j}^n + u_{i,j-1}^n \\[2mm]
(u_{xy})_{i,j}^n = \dfrac{u_{i+1,j+1}^n - u_{i-1,j+1}^n - u_{i+1,j-1}^n + u_{i-1,j-1}^n}{4}
\end{cases}
$$

(15)

$(u_{\xi\xi})_{i,j}^n$ and $(u_{\eta\eta})_{i,j}^n$ can be expressed by Eqs. (13) and (15). Let $\alpha = g(|\nabla u|)$, the discrete form of Eq. (12) is

$$
\begin{aligned}
u_{i,j}^{n+1} &= u_{i,j}^n + \Delta t \Big\{ (1 - \alpha_{i,j}^n)[\mu_1 (u_{\xi\xi})_{i,j}^n \\
&+ (\mu_2)_{i,j}^n (u_{\eta\eta})_{i,j}^n] + \alpha_{i,j}^n \\
&\cdot \frac{[(\alpha u_x)_{i+1,j}^n - (\alpha u_x)_{i-1,j}^n] + [(\alpha u_y)_{i,j+1}^n - (\alpha u_y)_{i,j-1}^n]}{2} \Big\}.
\end{aligned}
$$

(16)

The proposed method can be used in ESPI fringes. To validate the performance of the method, we test it on computer-simulated and practically captured fringes and compare it with the P-M diffusion and the tensor diffusion models.

Figure 1(a) shows a computer-simulated ESPI fringe[8], which is generated based on the following equation:

$$
I(x,y) = P(x,y) + Q(x,y)\cos\varphi(x,y) + N_A(x,y), \quad (17)
$$

where $P(x, y)$ is the background intensity, $Q(x,y)/P(x,y)$ is the fringe contrast, and $N_A(x, y)$ is the additive Gaussian white noise of the fringe patterns. $\phi(x,y)$ is related to a physical variable to be inspected. Let $P(x,y) \equiv 150$, and $Q(x,y) \equiv 80$, $\varphi(x,y)$ can be calculated as

$$
\varphi(x,y) = 22.5\pi \left[\left(\frac{x - M/2}{M/2}\right)^2 + \left(\frac{y - N/2}{N/2}\right)^2 \right], \quad (18)
$$

where M and N are the image row and column, respectively. In this study, we choose $M = 200$ and $N = 250$. The processed results are shown in Figs. 1(b)–(d), including the filtered results of the P-M diffusion, the tensor diffusion, and the proposed models, with $n = 80$, $\Delta t = 0.2$, and $k = 10$.

The experimentally obtained ESPI image, which depicts the derivative of the out-of-plane displacement of a steel plate, is shown in Fig. 2(a). The steel plate is rigidly clamped at its boundary and is subjected to a load. The tested results for Fig. 2(a) are shown in Figs. 2(b)–(d) with $n = 150$, $\Delta t = 0.2$, and $k = 10$.

As shown in Figs. 1(b) and 2(b), the image filtered by the P-M diffusion model is blurred severely. Some virtual structures appear in the filtered fringe of the tensor diffusion model, as shown in Figs. 1(c) and 2(c). Obviously, the proposed model performs significantly better in both noise reduction and edge protection than the other two diffusion models, as shown in Figs. 1(d) and 2(d).

At the same time, combining with the sine/cosine filter, we test the three models to the phase pattern, with $n = 90$, $\Delta t = 0.2$, and $k = 10$. The results are shown in Fig. 3. The filter result of our model is obviously better
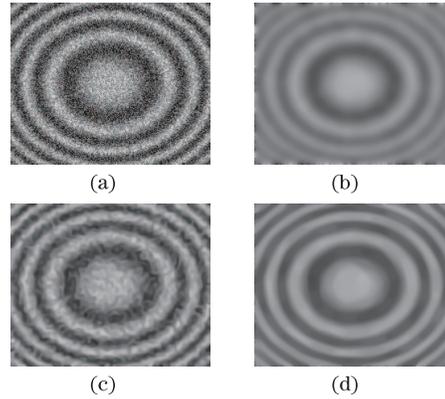

Fig. 1. Computer-simulated fringe and its filtered results. (a) Original computer-simulated fringe; filtered results of (b) the P-M diffusion, (c) the tensor diffusion, and (d) the proposed models.
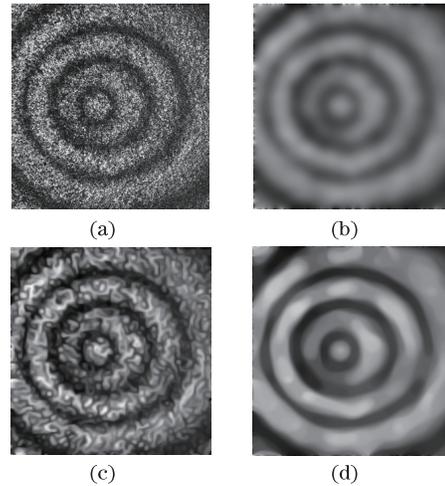

Fig. 2. Experimentally obtained fringe and its filtered results. (a) Original fringe; filtered results of (b) the P-M diffusion, (c) the tensor diffusion, and (d) the proposed models.
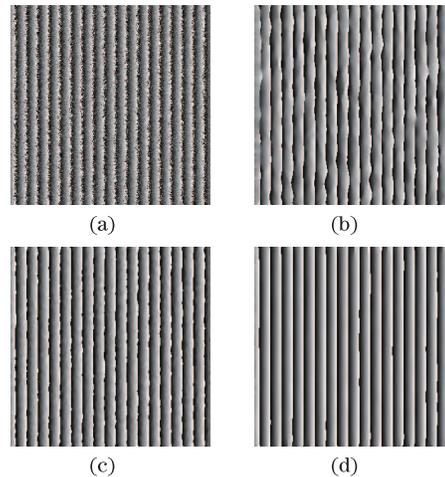

Fig. 3. Phase pattern and its filtered results. (a) Original phase pattern; filtered result of (b) the P-M diffusion, (c) the tensor diffusion, and (d) the proposed models.

than the former models and can keep the information of phase jump, while removing the inconsistent dots in the phase pattern effectively.

To measure quantitatively the performance of our model, two parameters, namely, fidelity and speckle index, are used to evaluate the filtering effect. Fidelity can be defined[9] as

$$f = 1 - \frac{\sum (I_0 - I)^2}{\sum I_0^2}, \tag{19}$$

where I is the processed fringe, and I_0 is the ideal non-noised fringe. A high fidelity value indicates that the processed image is very similar to the noiseless one, i.e., has a good fidelity.

The speckle index s is used to quantify the local smoothness of the filtered fringe patterns. This parameter is evaluated as the average of the ratios of the local standard deviation to its mean[9]:

$$s = \frac{1}{M \times N} \sum_{k=1}^{M} \sum_{l=1}^{N} \frac{\sigma_{k,l}}{\langle I_{k,l} \rangle}, \tag{20}$$

where $\langle I_{k,l} \rangle$ is the average gray in the neighborhood for a window of 3×3 pixels of the current point, and local standard deviation $\sigma_{k,l}$ is defined as

$$\sigma_{k,l} = \sqrt{\frac{1}{8} \sum_{i=-1}^{1} \sum_{j=-1}^{1} (I_{k-i,l-j} - \langle I_{k,l} \rangle)^2}. \tag{21}$$

The speckle index can be regarded as an average reciprocal of the signal-to-noise ratio, where the signal is the mean value, and the noise is the standard deviation. Therefore, a low speckle index will be regarded as an indication of the local smoothness of the fringe pattern.

We calculate f and s of each filtered results in Fig. 1, which are given in Table 1. Firstly, Table 1 shows that our model can give the largest fidelity among the three diffusion models under the same conditions. Given that the diffusion in our model is anisotropic based on the structural information, it has better edge protection capabilities. Secondly, our filter model can give obviously smaller s value than that of the tensor diffusion model. In addition, compared with the tensor diffusion model, our filtering model will not lead to virtual stripes, such that it can filter off noise more effectively. Thirdly, our filter model gives a little larger s value than that of the P-M diffusion model. This result may be caused by the large $\sigma_{k,l}$ value of the edge point (k, l) in our model, whereas the filtered result by the P-M diffusion model is

Table 1. Performance Evaluation of Three PDE Filter Models Based on Fringe Patterns in Fig. 1

Methods	f	s
P-M Diffusion Model	0.8333	0.0203
Tensor Diffusion Model	0.9079	0.0681
Our Diffusion Model	0.9225	0.0323

smoothed in both edge and inner fringe. These results prove that our model efficiently protects the structure of an image.

In conclusion, the advantages and disadvantages of the P-M diffusion and the tensor diffusion models are initially analyzed. An anisotropic PDE noise-reduction model based on coherence and P-M diffusions is then proposed. The proposed model is anisotropic based on the structure information of the image, which can repair the broken edges of the image and filter off the noise inside fringes effectively. The proposed method is tested on the fringe and phase patterns. The qualitative and quantitative results demonstrate that the proposed model has good noise reduction and edge protection capabilities. This model is an effective pre-processing method for ESPI fringe and phase patterns.

References

1. V. Bavigadda, R. Jallapuram, E. Mihaylova, and V. Toal, Opt. Lett. **35**, 3273 (2010).
2. N. A. Ochoa, F. M. Santoyo, A. J. Moore, and C. P. López, Appl. Opt. **36**, 2783 (1997).
3. B. G. Zogar, Chin. Opt. Lett. **9**, 071203 (2011).
4. F. Zhang, W. Liu, L. Xia, J. Wang, and Y. Zhu, Chin. Opt. Lett. **7**, 210 (2009).
5. P. Perona and J. Malik, IEEE Trans. Pattern Anal. Mach. Intell. **12**, 629 (1990).
6. J. Weickert, Acta. Math. Univ. Comenianae **LXX**, 33 (2001).
7. J. Weickert, Image Vis. Comput. **17**, 201 (1999).
8. F. Zhang, Z. T. Xiao, J. Wu, L. Geng, H. Q. Li, J. T. Xi, and J. J. Wang, Opt. Express **20**, 21905 (2012).
9. F. Zhang, W. Liu, J. Wang, Y. Zhu, and L. Xia, Opt. Commun. **282**, 2318 (2009).